

Ventral Visual Cortex in Humans: Cytoarchitectonic Mapping of Two Extrastriate Areas

Claudia Rottschy,^{1,2} Simon B. Eickhoff,^{1,2*} Axel Schleicher,²
Hartmurt Mohlberg,¹ Milenko Kujovic,² Karl Zilles,^{1,2,3}
and Katrin Amunts^{1,3,4}

¹*Institute of Medicine, Research Centre Jülich, Germany*

²*C. & O. Vogt Institute for Brain Research, University of Düsseldorf, Germany*

³*Brain Imaging Centre West, Research Centre Jülich, Germany*

⁴*Department of Psychiatry and Psychotherapy, RWTH Aachen University, Germany*

Abstract: The extrastriate visual cortex forms a complex system enabling the analysis of visually presented objects. To gain deeper insight into the anatomical basis of this system, we cytoarchitectonically mapped the ventral occipital cortex lateral to BA 18/V2 in 10 human postmortem brains. The anatomical characterization of this part of the ventral stream was performed by examination of cell-body-stained histological sections using quantitative cytoarchitectonic analysis. First, the gray level index (GLI) was measured in the ventral occipital lobe. Cytoarchitectonic borders, i.e., significant changes in the cortical lamination pattern, were then identified using an observer-independent algorithm based on multivariate analysis of GLI profiles. Two distinct cytoarchitectonic areas (hOC3v, hOC4v) were characterized in the ventral extrastriate cortex lateral to BA 18/V2. Area hOC3v was found in the collateral sulcus. hOC4v was located in this sulcus and also covered the fusiform gyrus in more occipital sections. Topographically, these areas thus seem to represent the anatomical substrates of functionally defined areas, VP/V3v and V4/V4v. Following histological analysis, the delineated cytoarchitectonic areas were transferred to 3D reconstructions of the respective postmortem brains, which in turn were spatially normalized to the Montreal Neurological Institute reference space. A probabilistic map was generated for each area which describes how many brains had a representation of this area in a particular voxel. These maps can now be used to identify the anatomical correlates of functional activations observed in neuroimaging experiments to enable a more informed investigation into the many open questions regarding the organization of the human visual cortex. *Hum Brain Mapp* 28:1045–1059, 2007.

© 2007 Wiley-Liss, Inc.

Key words: atlas; histology; V3; V4; V4v; VP; probabilistic maps

*Correspondence to: Simon B. Eickhoff, Institute of Medicine
Forschungszentrum Jülich GmbH, D-52425 Jülich, Germany.
E-mail: S.Eickhoff@fz-juelich.de

Received for publication 27 April 2006; Revision 21 July 2006;
Accepted 24 July 2006

DOI: 10.1002/hbm.20348

Published online 31 January 2007 in Wiley InterScience (www.
interscience.wiley.com).

© 2007 Wiley-Liss, Inc.

INTRODUCTION

The primate visual cortex can be differentiated into the striate cortex (the primary visual area, V1) receiving the mainstream of subcortical input (Alonso, 2002; Angelucci et al., 2002; Lund, 1988; Sherman, 2001; Worgotter and Eysel, 2000) and the surrounding extrastriate visual cortex which facilitates the further processing of visual

information. V1 is thought to mainly contain a direct representation of the retinal activation pattern, albeit low level feature processing (center-surround contrast, directivity columns) can already be found in this primary sensory area (Foster et al., 1985; Li et al., 2004; Smith et al., 2006; Victor et al., 1994). The adjoining extrastriate visual cortex, on the other hand, facilitates the more advanced analyses of visual information. It can be subdivided into two major processing axes: the dorsal and the ventral visual stream (Mishkin and Ungerleider, 1982; cf. review by Ettliger, 1990). The ventral stream is mainly involved in the identification and recognition of visually presented objects (including e.g., faces and words) based on features like color, texture and contours (Grill-Spector et al., 1998; Kanwisher et al., 1997; Malach et al., 2002). In contrast, the dorsal stream is particularly involved in spatial processing of visual information, e.g., in the context of eye–hand coordination (Fink et al., 2003; Grefkes et al., 2002; Roland et al., 1998; Weiss et al., 2000).

Orban et al. (2004) proposed a distinction of three hierarchical levels of integrational complexity in the primate visual cortex, which also correspond to different amounts of certainty regarding the homology between different primate species including humans. For early visual areas (V1, V2, V3), anatomical and functional homology between humans and nonhuman primates can be considered as largely proven (Conway and Tsao, 2006; Foster et al., 1985; Gallant et al., 1998; Haynes et al., 2005, but see Rosa and Manger, 2005). For midlevel visual areas (V3A, V4, MT) there is strong evidence for a largely preserved *regional* homology of their structural and functional organization (Hasnain et al., 1998; Larsson et al., 2006; Merriam and Colby, 2005). There is, however, some evidence suggesting that size, location or functional properties of at least some of these areas were modulated in the evolutionary course from monkeys to humans (DeYoe et al., 1996; Fize et al., 2003; Huk et al., 2002; Tsao et al., 2003). The homology of higher visual areas, e.g., those in the intraparietal sulcus and on the inferior temporal lobe still has to be examined in more detail, before conclusive inference on their homology within the primate family becomes feasible. Recent results do nevertheless favor a preserved regional homology between the humans and nonhuman primates also for higher order visual/polymodal areas of the posterior parietal cortex (Bremmer et al., 2001; Grefkes et al., 2002). It has to be noted though that the suggested distinction of visual areas into different classes of homologies within the primate family might very likely have to be revised again in the future based on functional and histological examination of further species (Rosa and Manger, 2005) and in particular based on further knowledge gained from performing more comparable imaging studies in humans and nonhuman primates, e.g., by means of monkey functional magnetic resonance imaging (fMRI) (Fize et al., 2003; Vanduffel et al., 2001).

In contrast to the detailed functional topography of the visual system which has been established for humans and

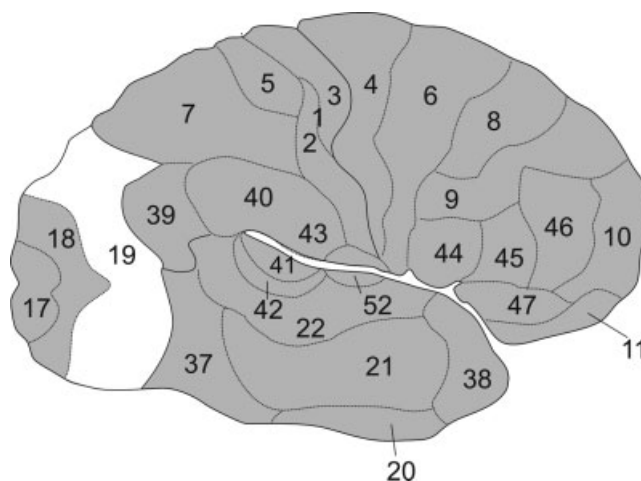


Figure 1.

Schematic view of Brodmann's areas (Brodmann, 1909). The cortex of the occipital lobe is only parcellated into three areas (Area 17, 18, 19). It becomes evident that BA 19 subsumes virtually all visual areas apart from V1 (BA 17) and V2 (BA 18).

nonhuman primates, most of the classical architectonic maps of the human brain only show a simple tripartition of the occipital lobe. Brodmann (Brodmann, 1909) and the succeeding Russian school (Sarkisov et al., 1949) for example described an area termed Brodmann area (BA) 17, representing the architectonic correlate of V1. This area is surrounded by BA 18, which in turn most likely corresponds to the functionally defined area V2 (Amunts et al., 2000). BA 18 is then followed by a single large area (BA 19), which covers both the ventral and dorsal aspect of the occipital cortex from the occipital–temporal gyrus to the parieto-occipital sulcus. That is, all visual areas apart from V1 and V2 seem to be included in the architectonic definition of BA 19. Von Economo and Koskinas also described a tripartition of the visual cortex (von Economo and Koskinas, 1925) consisting of area OC, which corresponds to BA 17/V1, area OB (the most likely correlate to BA 18/V2) and area OA, matching to Brodmann's area 19 in size and location. In contrast to Brodmann, however, they introduced “subregions” within this large occipital area, which were interpreted as local variations of a general architectonic pattern (Fig. 1).

It becomes evident, that these simplified maps will not serve as useful tools for the investigation of structure–function relationships in the human visual cortex. In addition to their overly coarse parcellation, all of these classical brain maps also share some important conceptual shortcomings impairing their combination with functional imaging data. For example, all classical anatomical brain maps only represent schematic two-dimensional drawings without any information about stereotaxic location and intersubject variability. Furthermore they are based on subjective criteria for the definitions of the borders of cortical

areas and only rarely provide information about cortical areas within the sulci (Zilles et al., 1988). A more detailed anatomical information is needed, which can then be integrated with data from functional imaging experiments, neurophysiological malfunction, and primate studies to elucidate the different organizational modules in the human (visual) cortex (cf. Eickhoff et al., 2005a; Passingham et al., 2002; Van Essen et al., 2000).

Probabilistic cytoarchitectonic maps (Amunts and Zilles, 2001; Eickhoff et al., 2005a; Zilles et al., 2002), on the other hand, provide a tool for more valid inferences about structure–function relationships in the human brain, since these maps are based on the observer-independent cytoarchitectonic analysis of 10 postmortem brains (Schleicher et al., 2005). They contain stereotaxic information about the location and variability of cortical areas in the Montreal Neurological Institute (MNI) reference space (Evans et al., 1992). The use of probabilistic cytoarchitectonic maps thus allows the examination of the microstructurally defined structural substrates of a cortical activation as measured by functional imaging experiments using fMRI, positron emission tomography (PET), or magnet-encephalography/electroencephalography (MEG/EEG) (Barnikol et al., 2006; Heim et al., 2005; Hurlemann et al., 2005; Larsson et al., 2002; Naito et al., 2005; Wilms et al., 2005; Young et al., 2004).

Our aim was therefore to reanalyze the cytoarchitecture of the early human ventral extrastriate cortex and to create three-dimensional probabilistic maps (Amunts et al., 2004; Eickhoff et al., 2005a; Mohlberg et al., 2003; Zilles et al., 2002, 2003) for the defined areas in standard stereotaxic space. These probabilistic cytoarchitectonic maps can then be used to compare activations of the ventral extrastriate cortex in imaging studies, with their anatomical correlates, and may enable the answering of some of the unresolved questions about the functional neuroanatomy of the human ventral extrastriate cortex.

MATERIALS AND METHODS

Histological Processing

Ten human postmortem brains (Amunts et al., 2000; Malikovic et al., in press) were obtained from body donor programs of the University of Düsseldorf (Table I). Only one brain came from a subject with transitory motor disturbances. All other subjects had no history of psychiatric or neurological diseases. Handedness of the subjects was unknown but since on average 10% of the population is left handed (Annett, 1973) we may assume that the majority was right handed. The brains were removed from the skull (postmortem delay <24 h) and fixed in 4% formalin or Bodian’s fixative for at least 6 months (Fig. 2A). To minimize distortions, the brains were suspended by the vertebral arteries to float freely in the fixative. After fixation, whole brain MR imaging was performed on a Siemens 1.5T scanner (Erlangen, Germany) with a T1-

TABLE I. Summary of the brains used for cytoarchitectonic analysis of the ventral occipital cortex

Case	Age (years)	Gender	Cause of Death
1	79	F	Carcinoma of the bladder
2	55	M	Rectal carcinoma
3	68	M	Vascular disease
4	75	M	Acute glomerulonephritis
5	59	F	Cardiorespiratory insufficiency
6	54	M	Cardiac infarction
7	37	M	Cardiac arrest
8	72	F	Renal failure
9	79	F	Cardiorespiratory insufficiency
10	85	F	Mesenteric infarction

weighted 3D FLASH sequence (flip angle 40°, repetition time TR = 40 ms, echo time TE = 5 ms for each image) for documentation of brain size and shape. Subsequently, the brains were embedded into paraffin, and serial whole brain sections (coronal plane) were obtained at 20 μ m. An image of the paraffin blockface was taken after every 60th section. Following cell body staining using a silver staining method (Merker, 1983) the sections corresponding to the obtained blockface images were examined, resulting in a gap of 1.2 mm between the analyzed sections.

Cytoarchitectonic Mapping

Regions of interest (ROIs) were defined on the ventral occipital cortex (Fig. 2B) and were digitized by a computer-controlled microscope, scanning the ROI in a meander-like sequence using a CCD camera. The digitized sections were converted to gray level index (GLI) images (Schleicher et al., 2000; Wree et al., 1982), which quantify the volume fractions of cell bodies in the corresponding measuring fields (Fig. 2C), to ameliorate differences in the staining intensity within and between sections (for further image acquisition and preprocessing details see (Amunts et al., 2000; Eickhoff et al., 2006c; Grefkes et al., 2001; Schleicher et al., 1999)).

The cortical ribbon was defined in the GLI-images by interactively tracing an outer contour between layers I and II, and an inner line between layer VI and the white matter. Curvilinear traverses, running perpendicular to the cortical layers from the outer to the inner contour (Fig. 2D), were automatically calculated based on the Laplace equation (Annese et al., 2004; Jones et al., 2000; Schleicher et al., 2005; Schmitt and Bohme, 2002). Along these traverses, profiles describing the changes in the laminar cell density pattern (Schleicher et al., 2000, 2005) were extracted from the GLI images. The shape of these profiles was quantitatively described using a 10 element feature vector, made up from the following parameters: mean GLI, cortical depth of the center of gravity, standard deviation, skewness, and kurtosis of the profile, as well as the analogous parameters for the absolute value of its first derivative (Amunts et al., 2000; Dixon et al., 1988; Zilles et al., 2002). Areal borders

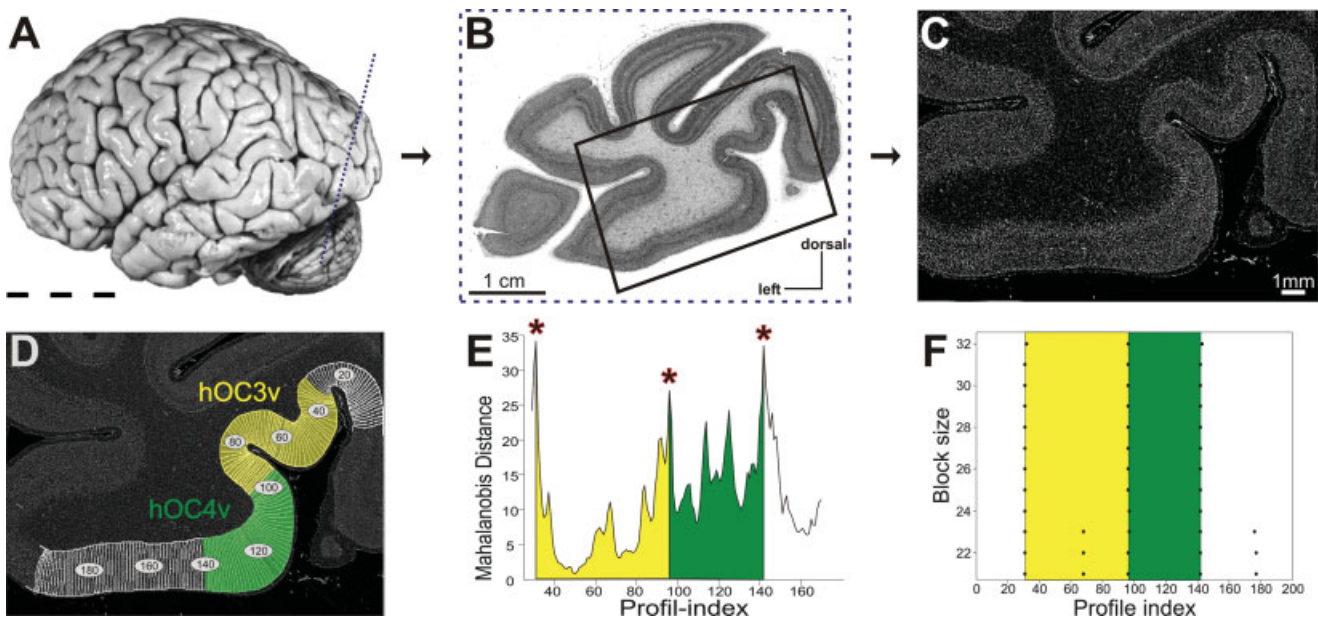


Figure 2.

Image acquisition and definition of cortical borders in cell-body-stained histological sections. **A:** Lateral view of postmortem brain 6, [cf. Table I]. The plane of sectioning of the histological section shown in (B) is marked by a dotted line. **B:** Cell body stained histological section of the left hemisphere through the occipital cortex of the brain shown in 2A. The box marks the region of interest (ROI) for the quantitative, cytoarchitectonic analysis detailed in (C)–(F). **C:** Gray level index (GLI) image of the ROI shown in (B). Each pixel corresponds to a certain

volume fraction of cell bodies in small measuring fields of $20 \times 20 \mu\text{m}^2$. **D:** The positions of the GLI profiles of the ROI are marked on the GLI image. The extent of area hOC3v (yellow) and area hOC4v (green) as defined by the cytoarchitectonic analysis (E)–(F) is shown. **E:** Mahalanobis distance function at blocksize 29. Significant maxima indicate cortical areas. They are marked by asterisks. **F:** Summary of the location of significant maxima over all examined block sizes. The location of borders does not vary in dependence on block size.

were subsequently identified at those profile positions where the layer pattern of the cortex changes significantly (Fig. 2E,F). To reveal such transitions, blocks of profiles were compared with the neighboring blocks using a sliding window algorithm (Schleicher et al., 2000, 2005). The dissimilarity between these blocks was quantified using the Mahalanobis distance (Mahalanobis et al., 1949) and were statistically tested using a Hotelling's T^2 -test (Bonferroni correction for multiple comparisons). This procedure was repeated for several block sizes to identify those borders that were consistent in spite of the inevitable noise in the images. The results of this observer-independent approach were then confirmed by a visual comparison with the histological sections and validated in a stack of neighboring sections (cf. Eickhoff et al., 2006c; Greffkes et al., 2001; Malikovic et al., in press; Morosan et al., 2001; Zilles et al., 2002).

Computation of Probabilistic Cytoarchitectonic Maps

The histological volumes of the brains were 3D reconstructed (Amunts et al., 2004; Mohlberg et al., 2003) using

the following three data sets available for each of the 10 postmortem brains: (i) The MRT scan, a 3D volume with only minor deformations but low spatial resolution. (ii) The blockface images, containing a reference grid to establish the integrity of the data set orthogonal to the cutting plane. (iii) Digitized images of the cell body stained sections. These images show the most detailed anatomical information but are highly deformed and contain no spatial reference. The defined areas were then interactively transferred to the respective sections of the reconstructed volume.

The reconstructed postmortem brains were then spatially normalized to the T1-weighted single-subject template of the MNI (Evans et al., 1992) using a nonlinear elastic registration algorithm (Amunts et al., 2004; Henn et al., 1997; Hömke, 2006; Mohlberg et al., 2003). The origin of the MNI reference space, however, does not coincide with the location of the anterior commissure (AC) of this specific template brain but is located 4 mm more caudally (y -axis) and 5 mm more dorsally (z -axis). To keep the AC as the anatomical reference of the coordinate system, the origin of the cytoarchitectonic maps was corrected for this displacement. The maps are thus registered in the

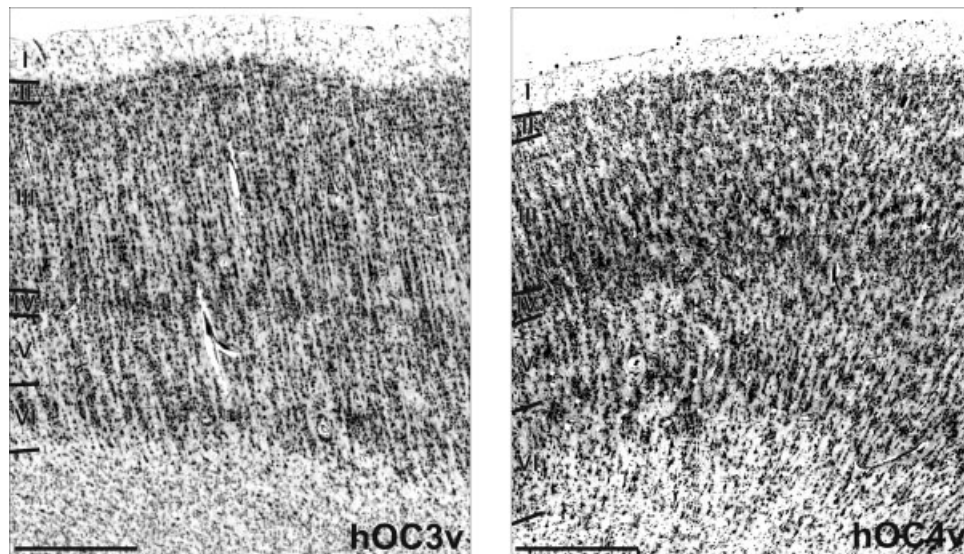


Figure 3.

Overview of the cytoarchitecture of hOC3v and hOC4v. Area hOC3v is characterized by a fine columnar arrangement of its cells, an inconspicuous layer IV and the absence of prominent pyramidal cells in deeper layer III. Area hOC4v on the other hand shows a high amount of larger pyramidal cells in deeper layer III, more prominent layers IV and VI as well as a border columnar arrangement. Roman numerals denote cortical layers, bar: 1 mm.

'anatomical MNI space' (Amunts et al., 2005; Eickhoff et al., 2005a), which differs from the original MNI space only by the linear shift of the origin. Following spatial normalization, the corresponding areas of the different subjects were superimposed and a probabilistic map was generated for each area (Eickhoff et al., 2006b). It describes, for each voxel of the reference brain, how many individual brains overlapped with the respective cytoarchitectonic area in that particular voxel.

Quantitative Analysis of Volumes and Stereotaxic Location

The volumes of areas hOC3v and hOC4v were then analyzed with respect to interhemispheric and interareal differences by a two-way analysis of variance (ANOVA) using the following design: the two factors were 'hemisphere' (left, right) and 'area' (hOC3v, hOC4v); the blocking factor was 'brain'. The level of significance was $P < 0.05$. If the effect of a factor was significant, we used a subsequent pairwise multiple comparison procedure (Tukey test) to isolate the conditions in which the levels of this factor differed significantly ($P < 0.05$).

Interhemispheric differences in the stereotaxic location of hOC3v and hOC4v with respect to the anterior-posterior, the medial-lateral, and the inferior-superior axes were tested by using the same procedure.

Cytoarchitectonic Probability Maps and Maximum Probability Map

As described in the section "Computation of Probabilistic Cytoarchitectonic Maps", probabilistic maps were generated for hOC3v and hOC4v as well as for V1, V2 (Amunts et al., 2000), and hOC5 (Malikovic et al., in press). A maximum probability map (MPM) of all these areas, i.e., a summary map of all early ventral visual areas defined to date, was computed by comparing the probabilities for each area (i.e., the numbers of overlapping representations) in each voxel (Eickhoff et al., 2005a) and assigning each voxel to the most likely anatomical area. If different areas showed equally high probabilities for occurring in the same voxel, this voxel was assigned to that area which showed the higher average probability in the 26 directly adjacent voxels. To evaluate the quality of representation, volumes and locations of the MPM representations were subsequently compared with the mean values for the respective area after normalization.

RESULTS

Two distinct cytoarchitectonic areas were identified in the ventral extrastriate human visual cortex lateral to BA 18 (see Fig. 3). Adopting a neutral nomenclature to avoid a premature implication of correspondence with functionally defined regions, these areas were named hOC3v and hOC4v (h, human; OC, occipital cortex; v, ventral).

hOC3v is located immediately lateral to the ventral part of BA 18/V2. It was found in the collateral sulcus in all the 20 examined hemispheres. More laterally, a second area was identified which directly bordered hOC3v over its full length. This area (hOC4v) was located in the collateral sulcus in the more frontal sections, but also covered large parts of the fusiform gyrus in the more occipital sections in all the 20 hemispheres. Both hOC3v and hOC4v were mainly located on the ventral aspect of the occipital lobe, but also occupied parts of its lateral surface close to the occipital pole.

The cytoarchitecture of area hOC3v differs from that of BA 18/V2 (Amunts et al., 2000) in many aspects; area hOC3v is characterized by distinct cell columns which are less present in BA 18. Although layer II of area hOC3v is only moderately cell dense without a clear border to layer III, these layers are clearly distinguished in BA 18 (Fig. 4A). Area hOC3v has a rather cell sparse layer III without a marked increase in the size of pyramidal cells from sublayer IIIa to sublayer IIIc. In contrast, BA 18 has a more cell dense layer III and features distinctly large pyramidal cells in layer IIIc. Although layer IV of hOC3v only shows a moderate cell density (rendering its transition to layer V rather inconspicuous), layer IV of BA 18 shows a clearly higher cell density and has a well defined border to a cell sparse layer V. Finally, both the layers V and VI are more cell sparse in BA 18, when compared with hOC3v.

In the most occipital sections, hOC3v also borders an area which follows the dorsal part of BA 18. Following the neutral nomenclature used throughout this correspondence, this area which putatively represents the structural substrate of functionally defined area V3 (or V3d) (Zeki, 1969a) will be labeled hOC3d. The external granular cell layer (layer II) is distinctly less cell dense in area hOC3d than in hOC3v. Although an increase of the size of pyramidal cells within layer III is seen in both areas (hOC3d and hOC3v), the number of large pyramidal cells is smaller in hOC3d than in hOC3v (Fig. 4B). In area hOC3d, layer IV is more cell sparse and has a better defined border to layer V. Furthermore, layers V and VI are similarly cell dense in area hOC3d, resulting in an inconspicuous border between these layers. In hOC3v, on the other hand, layer V contains markedly fewer and smaller cells than layer VI, resulting in a better separation of these two layers.

Area hOC4v is found lateral to hOC3v on the lateral bank of the collateral sulcus and on the fusiform gyrus. Compared with area hOC3v, hOC4v is characterized by a more cell dense layer II and a much more pronounced increase of density and size of pyramidal cells throughout layer III. In contrast to hOC3v, layer IV is very prominent in area hOC4v (Fig. 5A). The higher cell packing density in the inner granular layer (layer IV) provided one of the main features for the differentiation between hOC3v and hOC4v. The absolute cell density within both the layers V and VI is higher in hOC4v than in hOC3v, although layer V of hOC4v shows only few large pyramidal cells.

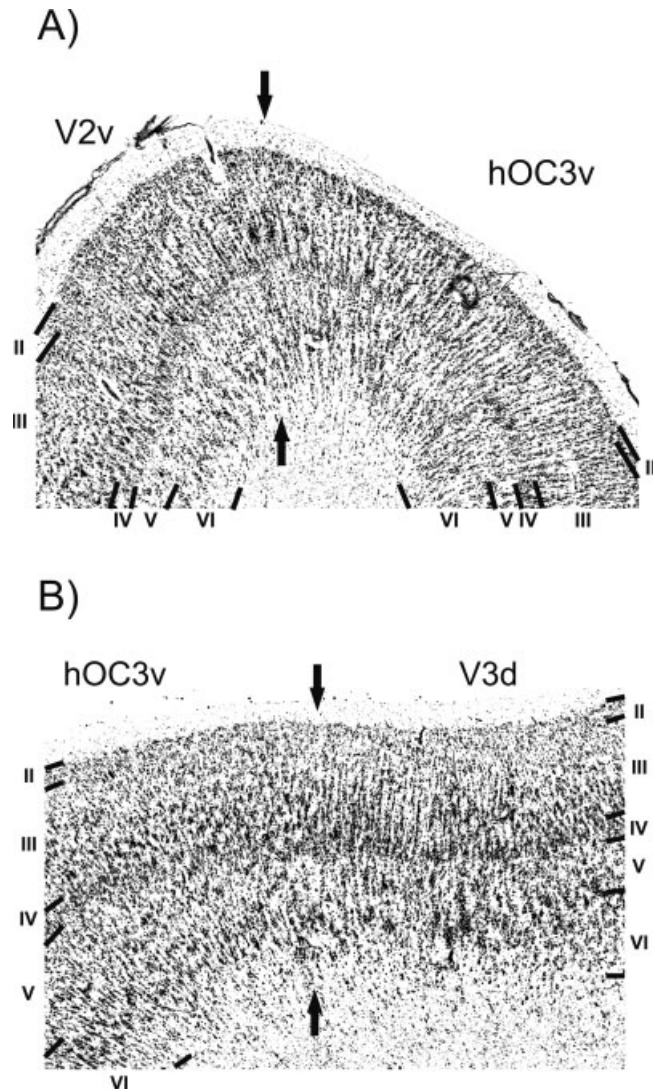


Figure 4.

A: Border between area hOC3v and area hOC3d. This border is marked by a decrease in the size of pyramidal cells in layer III in hOC3v. Furthermore hOC3v is characterized by a less cell dense layer IV and the presence of distinct cell columns not present to the same degree in area V2. Roman numerals denote cortical layers; bar, 1 mm. **B:** Border between area hOC3v and area hOC3d/V3d. It is characterized by a further decline in the size of pyramidal cells in layer III in hOC3d compared with hOC3v and by a more pronounced columnar arrangement in hOC3d.

The cortex lateral to hOC4v (putatively corresponding to functionally defined V4d (Tootell and Hadjikhani, 2001), the lateral occipital cortex (LOC) (Malach et al., 1995), and the fusiform face area (FFA) (Kanwisher et al., 1997)) features more pronounced cell columns than area hOC4v. The transition between layers II and III is less well defined,

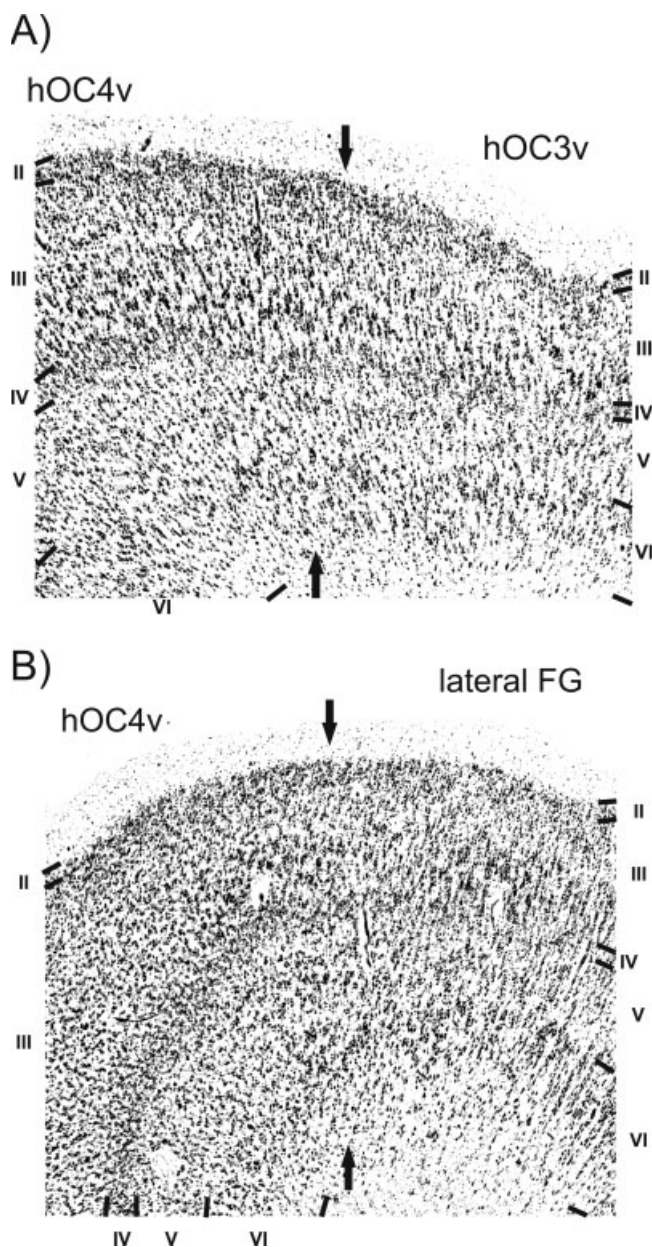


Figure 5.

A: Border between hOC3v and hOC4v. In comparison to hOC3v, hOC4v shows an increase in the size and amount of pyramidal cells in layer III and also features a wider and more cell dense layer IV. Roman numerals denote cortical layers; bar, 1 mm. **B:** Border between hOC4v and the cortex lateral to this area on the fusiform gyrus (FG). In the area on the lateral fusiform gyrus the inner granular layer (IV) is less thick and of lower cell density. Layer III is also less cell dense in that lateral area and contains only small pyramidal cells.

and layer III is more cell sparse when compared with hOC4v (Fig. 5B). Furthermore, the increase in the size of pyramidal cells within layer III is much more pronounced

in hOC4v. Layer IV shows the most pronounced differences, as it is considerably thicker and more cell dense in hOC4v when compared with the cortex lateral to it. Layer V of the cortex following lateral to hOC4v is rather cell sparse and has a clear border to layer VI. Since both the layers V and VI feature similarly high cell packing densities in hOC4v, the border between these layers is less well defined in this latter area. Finally, the cortex–white matter border is less well defined in the cortex lateral to hOC4v than in hOC4v.

Volumes and Stereotaxic Localization of Areas hOC3v and hOC4v

There was a high intersubject variability in size and location of both areas (Table II). The volumes of hOC3v, for example, ranged from 4447 mm³ to 13,707 mm³ among brains. In the statistical analysis, no volume differences were found between the two hemispheres for either area (no significant interaction between the factors area and side: $F = 0.34$, $P > 0.05$). Similarly, there was no statistically significant difference in the mean volumes between hOC3v and hOC4v after allowing for effects of interindividual variations (effect of factor area: $F = 2.12$, $P > 0.05$).

The coordinates for the centers of gravity of hOC3v and hOC4v in anatomical MNI space are given in Table III. Significant interhemispheric differences in the medial–lateral and anterior–posterior location were observed for both hOC3v and hOC4v. In detail, both areas were located more laterally and anterior in the right hemisphere ($F_{ML} = 11.75$, $F_{AP} = 7.45$, $P < 0.05$), a fact which might be explained by the marked asymmetry of the occipital pole of the MNI single subject template. There was, however, no difference in location of either area along the ventral–dorsal axis ($P > 0.05$).

TABLE II. Volume measurements of the ventral extrastriate cortex

	hOC3v	hOC4v
Raw volumes		
Right hemisphere	8640 ± 2180	6361 ± 1521
Left hemisphere	8475 ± 2014	7407 ± 2494
Total volume	17115 ± 3492	13768 ± 3206
Normalized volumes		
Right hemisphere	7897 ± 1333	5566 ± 1025
Left hemisphere	7839 ± 1310	6905 ± 1973
Total volume	15736 ± 2483	12472 ± 2618

For each area, its mean volume (±SD) on the right and left hemisphere as well as its mean total volume (±SD) are given in mm³. Raw volume data have been obtained by volumetric measurements from the reconstructed histological volumes prior to any linear or nonlinear normalization. Normalized volume data have been calculated after linear or nonlinear warping to the MNI single subject template.

TABLE III. Coordinates of the centers of gravity of hOC3v and hOC4v (mean \pm SD across the 10 subjects after nonlinear normalization) as well as the centers of gravity for the corresponding MPM representations

	X	Y	Z
Left hemisphere			
hOC3v	-19.8 ± 5.0	-87.9 ± 3.9	-1.12 ± 2.4
MPM	-20.1	-88.2	-3.1
hOC4v	-26.2 ± 4.6	-82.7 ± 5.2	-4.9 ± 1.9
MPM	-29.0	-84.4	-7.4
Right hemisphere			
hOC3v	24.4 ± 2.7	-83.7 ± 3.7	-2.3 ± 1.6
MPM	25.6	-84.3	-3.7
hOC4v	31.0 ± 4.7	-79.3 ± 4.8	-5.2 ± 0.9
MPM	33.9	-79.6	-7.6

All locations are given in anatomical MNI space (Eickhoff et al., 2005a).

Probability Maps of the Ventral Extrastriate Cortex

Probabilistic cytoarchitectonic maps in the anatomical MNI reference space were computed for hOC3v and hOC4v (Figs. 6 and 8). These maps showed that high probabilities, corresponding to locations where a specific area was found in, e.g., 9 out of 10 examined brains, were only observed for a small number of voxels. In contrast, the volumes for low probabilities, e.g., made up by a voxel containing an area in 2 out of 10 brains, were considerably larger. As a consequence, the probabilistic maps of hOC3v, hOC4v, BA 17, and BA 18 overlapped considerably at lower probabilities, i.e., it was impossible to assign all voxels in the ventral occipital cortex unequivocally to a specific cytoarchitectonic area at lower thresholds.

In contradistinction, the MPM of the early visual areas (Figs. 7 and 8) (Amunts et al., 2000) represents a contiguous, nonoverlapping parcellation of the occipital cortex. Importantly the MPM does not show the parcellation of an exemplary or ‘typical’ hemisphere as do classical architectonic brain maps (e.g., Brodmann, 1909), but reflects the most likely area at each position in a sample of 10 post-mortem brains.

In total, 23,622 voxels (1 mm^3 each) were assigned to either hOC3v or hOC4v in the computed MPM of the early visual cortex. This corresponds to a volume representation of approximately 85% relative to the mean areal volumes after nonlinear normalization, i.e., the MPM representations of hOC3v and hOC4v were approximately 15% smaller than the average size of the respective areas after normalization. This deviation from the mean volume is thus in the same range as observed for MPM representations of other cortical areas (Eickhoff et al., 2006b). There is also a good match in stereotaxic location between hOC3v and hOC4v and their representations in the MPM (Table II). All but two (z-location of area hOC4v) coordinates

for the centers of gravity of the MPM representations are located within only one standard deviation of the mean coordinates of the respective area.

DISCUSSION

This study reports two distinct architectonic areas in the ventral extrastriate human visual cortex lateral to BA 18 (hOC3v and hOC4v), which were identified using classical histological criteria and quantitative cytoarchitectonic analysis (Schleicher et al., 1998, 2005). The application of a statistical approach for the detection of areal borders represent an important difference from the classical cytoarchitectonic examinations (e.g., Brodmann, 1909; Sarkisov et al., 1949; von Economo and Koskinas, 1925), which relied purely on the visual inspection of histological sections and were thus largely subjective. Area hOC3v is located in the collateral sulcus; hOC4v is found on the lateral bank of this sulcus but also reaches the fusiform gyrus in the occipital sections. To interpret the cytoarchitectonic entities, they have to be related to previous architectonic maps of the human occipital cortex, results of nonhuman primate research, and human functional imaging studies.

Comparison With Previous Architectonic Maps

Classical anatomical brain maps mainly show a tripartition of the ventral extrastriate cortex (Brodmann, 1909; Sarkisov et al., 1949). Only von Economo and Koskinas, whose area OA corresponds to the extrastriate visual cortex anterior to BA 18/V2, mapped regional variations in the cytoarchitectonic features of these areas (von Economo and Koskinas, 1925). That is, they described architectonic differences between the dorsal, lateral, and ventral parts of area OA, which may correspond to the differentiation between the dorsal and ventral streams, as well as the higher order visual areas on the lateral occipital lobe. In particular, the differentiation between subareas OAm (ventral) and OA2 (dorsal) and OA (lateral) may very well correspond to the described differences between the ventral extrastriate areas hOC3v/hOC4v, hOC3d and the LOC, respectively, although the locations of the borders between these subregions were not indicated by von Economo and Koskinas. Differences within the ventral extrastriate cortex, however, corresponding to the differentiation between hOC3v and hOC4v, were not described.

Brodmann’s area 19 has later been reinvestigated using myeloarchitectonic (Clarke and Miklossy, 1990) and cytoarchitectonic criteria (Clarke et al., 2000; Zilles and Clarke, 1997). In these studies, the area following BA 18 in the ventral stream of the extrastriate cortex (termed area VP) is described as follows: “VP is lightly myelinated and lacks the large pyramids in layer III. The cortex lateral to VP is heavily myelinated and contains fairly large pyramids in layers III and V.” This description is thus similar to our cytoarchitectonic characterization of area hOC3v and hOC4v. Moreover, the size and location of area VP and its

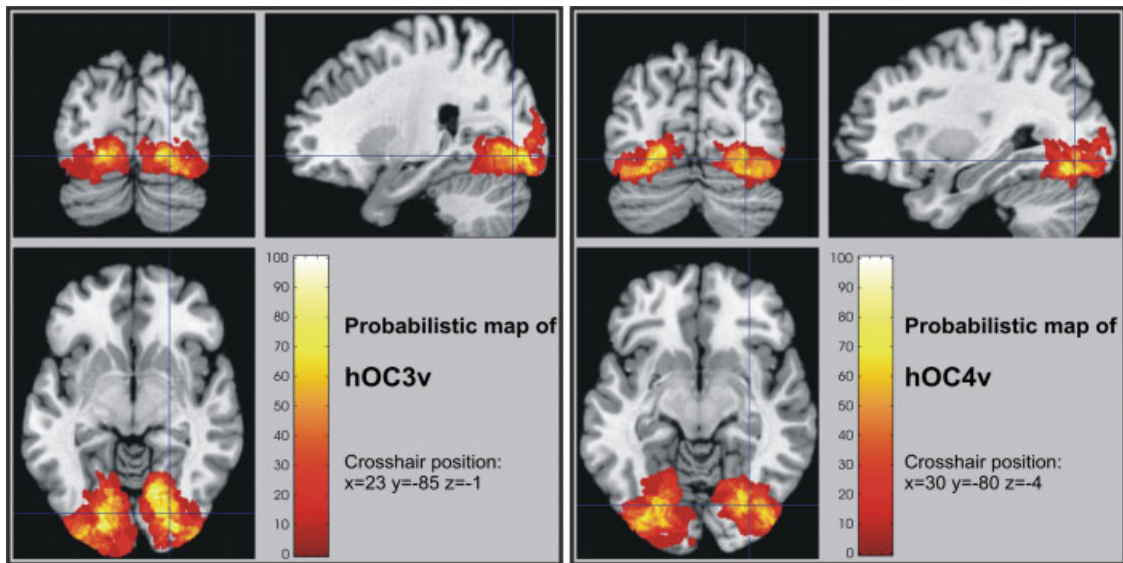


Figure 6.

Orthogonal sections through the probabilistic maps of hOC3v and hOC4v in anatomical MNI space. The relative probabilities for observing the respective areas at each voxel of the reference space is color-coded from dark red (low probability) to white (high probability).

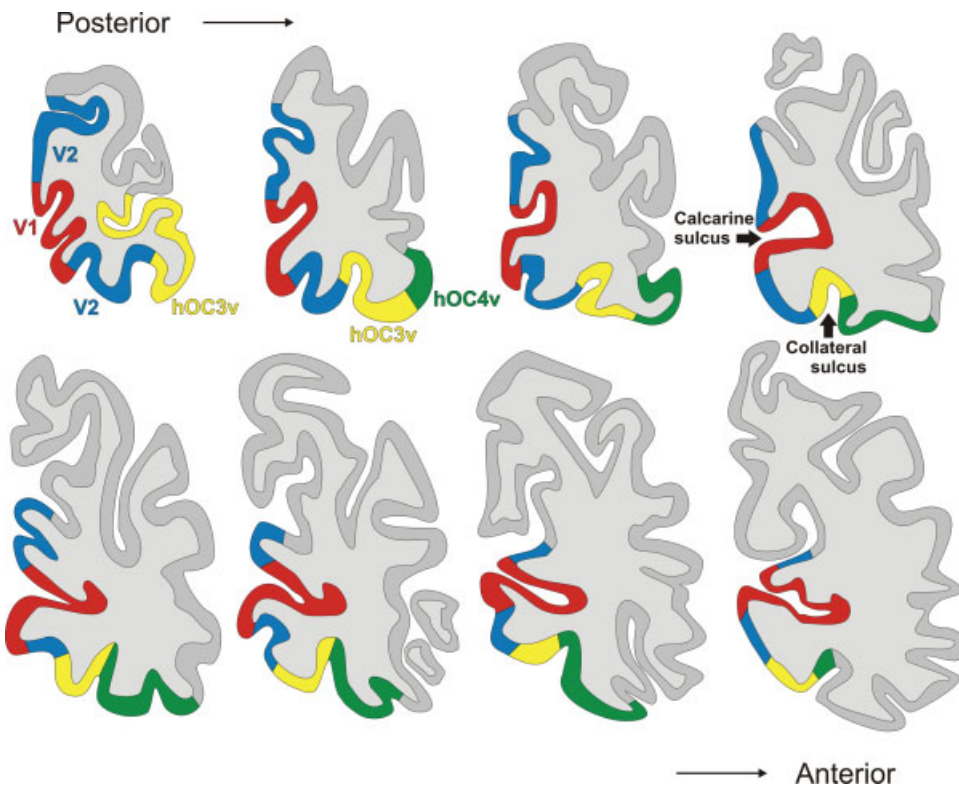


Figure 7.

The displayed maximum probability map (MPM) of the visual cortex includes the two ventral areas described in this paper as well as areas V1 and V2 (Amunts et al., 2000) and is shown on the right hemisphere of the MNI single subject template. In this series of coronal sections, the upper left image represents the most posterior section, while the lower right image is the most

anterior one. Both areas hOC3v and hOC4v are located in the region of the collateral sulcus. hOC4v also covers the fusiform gyrus in the more caudally located sections. (Red, area 17/V1; blue, ventral and dorsal part of area 18/V2; yellow, area hOC3v on the collateral sulcus; green, area hOC4v within the collateral sulcus and on the fusiform gyrus.)

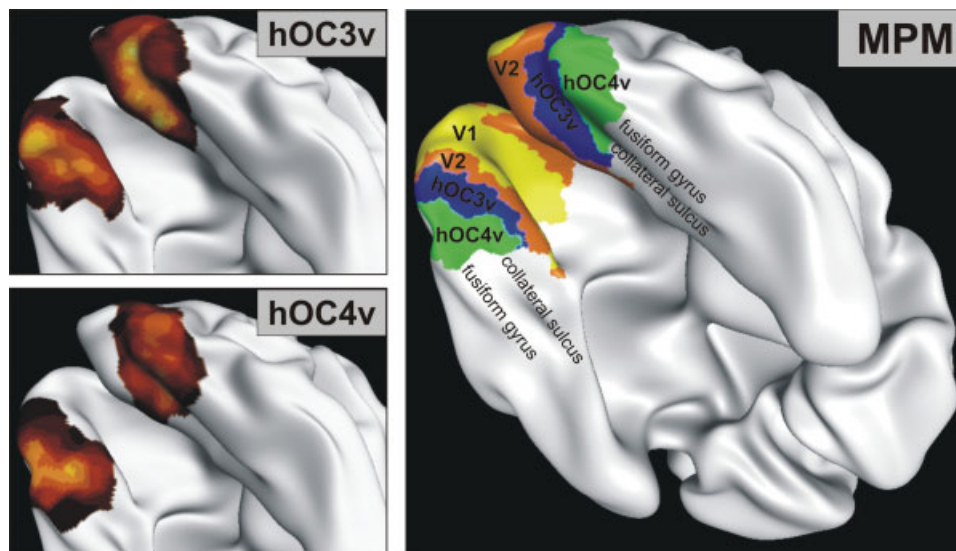


Figure 8.

Visualization of the cytoarchitectonic probability maps for hOC3v (left, top) respectively hOC4v (left, bottom) and the maximum probability map (MPM) of the visual cortex including V1, V2, hOC3v, and hOC4v on the reconstructed and inflated surface of the MNI single subject brain. This view, which is also

commonly used for visualization of functional imaging results, again demonstrates the topology of the defined ventral visual areas. Area hOC3v is located in the collateral sulcus; hOC4v is found on the lateral bank of this sulcus but also reaches the fusiform gyrus in the occipital sections.

lateral neighbor correspond to our findings on areas hOC3v and hOC4v as well. Supplementing the data of Clarke et al., we here report probabilistic maps of hOC3v and hOC4v which represent a major advance, since this information can now directly be correlated with functional imaging results in order to characterize structure–function relationships (Eickhoff et al., 2005a).

Comparison With Data from Nonhuman Primates

Electrophysiological, tracing, and histological studies of nonhuman primates (Cavada and Goldman-Rakic, 1993; Felleman et al., 1997) as well as fMRI studies in these species (Orban et al., 2004) revealed a much more complex organization of the extrastriate cortex as described in classical *human* maps. The ventral part of BA 18 is followed by a smaller area in the collateral sulcus, either termed VP (Van Essen et al., 2001) or ventral V3 (V3v) (Desimone and Ungerleider, 1986; Zeki, 1969b). The dorsal part of V2, on the other hand, is followed by area V3 (or its dorsal part V3d in the alternate nomenclature defining the ventral neighbor of V2 as area V3v) (Boussaoud et al., 1991; Felleman and Van Essen, 1991). In this context, it is important to point out that areas VP or V3v are almost identical in size and location. Thus, rather than denoting two distinct areas, these terms express different views about the functional relationship between this ventral extrastriate area to its dorsal counterpart. Although some authors have

shown functional differences between VP and dorsal V3 in macaques, e.g., in the response to color stimuli (Burkhalter et al., 1986; Felleman and Van Essen, 1987) and thus coined the term VP, this view was contradicted by others, who did not find such functional differences and argue that V3v and V3d jointly contain a single representation of the visual world and are thus parts of a single area (e.g., Gardner et al., 2005; Wade et al., 2004; Zeki, 1978a).

Comparison of the size and location of primate areas VP/V3v to area hOC3v as defined by cytoarchitectonic mapping in human postmortem brains reveals that hOC3v is topologically equivalent to VP/V3v. This supports the notion of close homology between monkeys and humans for early visual areas (Conway and Tsao, 2006; Foster et al., 1985; Haynes et al., 2005). However, the fact that we described architectonic differences between hOC3v and the area which follows BA 18/V2 dorsally may be seen as evidence for a differentiation between the dorsal and ventral visual cortex anterior to BA 18/V2 at least in humans.

The area, which laterally borders VP/V3v over its entire extent, was originally termed “V4” by Zeki (1969b) and is well studied for filtering properties (Desimone and Schein, 1987), color (Van Essen and Zeki, 1978; Zeki, 1978b), models of visual processing (Girard et al., 2002), and extraretinal modulation (Moran and Desimone, 1985) in macaque monkeys. In comparison to area V4 (Zeki, 1978a) in non-human primates, human area hOC4v is found at an almost identical position, but appears to be considerably smaller in size with respect to the whole extend of the visual

cortex. Although area V4 in monkeys covers the entire fusiform gyrus and extends up to the inferior temporal lobe, human area hOC4v covers the lateral bank of the sulcus collateralis and reaches only the fusiform gyrus in the occipital sections.

Based on electrophysiological and connection evidence from macaque monkeys (Felleman and Van Essen, 1991) as well as recent fMRI studies (Orban et al., 2004; Sereno et al., 1995), it has been suggested that V4 may be divided into a ventral part (V4v), located next to VP/V3v, and a dorsal part (V4d) located on the LOC. Because V4v covers only the collateral sulcus and the medial aspect of the fusiform gyrus, it appears to be more consistent with the extent of human area hOC4v than area V4, although the large interspecies differences in the relative sizes of visual cortical areas (Van Essen et al., 2001) render such comparisons very difficult and point to the need of further research in this direction.

Comparison With Human Functional Imaging Data

One of the most commonly used techniques for the functional delineation of visual areas is the application of retinotopic mapping (DeYoe et al., 1996; Engel et al., 1997; Grill-Spector et al., 1998; Sereno et al., 1995; Warnking et al., 2002). Hereby a cortical area can be defined on the basis of changes in the visual field sign and characterized as containing either the representation of a single quadrant of the contralateral visual scene or a complete hemifield. For the ventral extrastriate cortex, however, this method has provided slightly conflicting results; some authors stated that VP/V3v is followed by a retinotopic quadrant representation in an area corresponding to area V4v in other primates. This (upper) quadrant representation in V4v is matched by a representation of the contralateral lower visual quarterfield within neighboring area V4d. Anterior to V4v, a further complete hemifield representation was postulated (Tootell and Hadjikhani 2001). In contrast, Zeki et al. (1998) described VP/V3v as the last retinotopic quadrant representation in the ventral visual stream. This quadrant representation is then followed by a complete hemifield representation in area V4 (Zeki et al., 1998).

In this context, it is important to note that our data shows that hOC3v (i.e., VP/V3v) and hOC3d (V3d) constitute two distinct *cytoarchitectonic* areas. On the other hand, retinotopic mapping clearly demonstrated that area VP/V3v only contains a representation of the contralateral upper quarterfield, whereas V3d contains the matching lower quarterfield representation (Engel et al., 1997; Grill-Spector et al., 1998; Warnking et al., 2002). These studies therefore suggest that VP/V3v and V3d are both part of a single visual area, since bilateral VP/V3v (upper quadrants) and V3d (lower quadrants) contain a single complete representation of the whole visual world.

This discrepancy raises some important questions: Why are upper and lower visual fields represented in architectonically different parts of the cortex? Which functional differences, if any, correspond to these architectonic differences? Are such architectonic and functional differences related to the fact that different parts of the visual world (upper vs. lower field) are represented in the dorsal respective ventral visual cortex? A promising approach to answer these questions and to gain further insight into the organization of the early visual cortices may be provided by a multimodal approach which combines anatomical data such as receptor architectonic investigations (Hurlemann et al., 2005; Zilles et al., 2004), cytoarchitectonic mapping (Amunts et al., 2000; Malikovic et al., in press), structural MR imaging (Walters et al., in press; Eickhoff et al., 2005b), retinotopic mapping (Tootell et al., 1997), and functional imaging experiments (Larsson et al., 2002; Wilms et al., 2005) in a common analysis framework.

Such integration of anatomical and functional data (Eickhoff et al., 2005a) will also help to further characterize the cortex lateral to VP/V3v, i.e., the functional equivalent to hOC4v. This region (commonly termed V4) is supposed to be strongly responsive during segregated texture stimuli in comparison to uniform textures (Kastner et al., 2000). This is in good agreement to lesion studies in nonhuman primates showing that lesions in area V4 appear to disrupt only those texture discriminations that require grouping of similar elements to form a pop out (Merigan, 2000). The part of V4 that was termed V4v by some authors (Orban et al., 2004) was also reported to show an increase of activation in particular when contour stimuli are presented (Schira et al., 2004). However, as outlined earlier, the existence of V4v (quadrant representation) as opposed to an area V4 (hemifield) is in itself still a matter of conjecture. Similarly, there is an ongoing debate whether V4v is part of the human color selective region V4 (McKeefry and Zeki, 1997; Zeki et al., 1991) or whether the color center in the human visual cortex is located anterior to V4v and should then be termed V8 (Hadjikhani et al., 1998).

CONCLUSIONS

The presented study investigated the microstructural organization of the early ventral extrastriate visual cortex. In contrast to classical anatomical maps (e.g., that of Brodmann (1909)) which only show a schematized image of the brain's surface, our probabilistic maps are provided in standardized three-dimensional stereotaxic space. Therefore, it is now possible to combine these cytoarchitectonic data with statistical activation maps from fMRI (Wilms et al., 2005) and PET (Hurlemann et al., 2005) experiments or with equivalent dipoles from MEG or EEG studies (Barnikol et al., 2006). This integrated analysis of structure and function of the early ventral visual stream will then provide new and detailed answers to the many pending

questions, e.g., the relationship between VP/V3v and V3d or the location of the human color center.

To encourage the use of probabilistic cytoarchitectonic maps of hOC3v and hOC4v in the context of functional imaging experiments, these maps, together with a software tool (Eickhoff et al., 2005a) for integration into the widely used functional image analysis software SPM (The Wellcome Department of Imaging Neurosciences, www.fil.ion.ucl.ac.uk/SPM) are freely available at http://www.fz-juelich.de/ime/spm_anatomy_toolbox. MINC format versions of the described maps are also available at <http://www.bic.mni.mcgill.ca/cytoarchitectonics/>.

ACKNOWLEDGMENTS

This Human Brain Project/Neuroinformatics research was funded jointly by the National Institute of Mental Health, of Neurological Disorders and Stroke, of Drug Abuse, the National Cancer Centre and the Deutsche Forschungsgemeinschaft (KFO-112).

REFERENCES

- Alonso JM (2002): Neural connections and receptive field properties in the primary visual cortex. *Neuroscientist* 8:443–456.
- Amunts K, Malikovic A, Mohlberg H, Schormann T, Zilles K (2000): Brodmann's areas 17 and 18 brought into stereotaxic space—Where and how variable? *Neuroimage* 11:66–84.
- Amunts K, Zilles K (2001): Advances in cytoarchitectonic mapping of the human cerebral cortex. *Neuroimaging Clin N Am* 11:151–169, vii.
- Amunts K, Weiss PH, Mohlberg H, Pieperhoff P, Eickhoff S, Gurd JM, Marshall JC, Shah NJ, Fink GR, Zilles K (2004): Analysis of neural mechanisms underlying verbal fluency in cytoarchitectonically defined stereotaxic space—The roles of Brodmann areas 44 and 45. *Neuroimage* 22:42–56.
- Amunts K, Kedo O, Kindler M, Pieperhoff P, Mohlberg H, Shah NJ, Habel U, Schneider F, Zilles K (2005): Cytoarchitectonic mapping of the human amygdala, hippocampal region and entorhinal cortex: Intersubject variability and probability maps. *Anat Embryol (Berl)* 210:343–352.
- Angelucci A, Levitt JB, Lund JS (2002): Anatomical origins of the classical receptive field and modulatory surround field of single neurons in macaque visual cortical area V1. *Prog Brain Res* 136:373–388.
- Annese J, Pitiot A, Dinov ID, Toga AW (2004): A myeloarchitectonic method for the structural classification of cortical areas. *Neuroimage* 21:15–26.
- Annett M (1973): Handedness in families. *Ann Hum Genet* 37:93–105.
- Barnikol UB, Amunts K, Dammers J, Mohlberg H, Fieseler T, Malikovic A, Zilles K, Niedeggen M, Tass PA (2006): Pattern reversal visual evoked responses of V1/V2 and V5/MT as revealed by MEG combined with probabilistic cytoarchitectonic maps. *Neuroimage* 31:86–108.
- Boussaoud D, Desimone R, Ungerleider LG (1991): Visual topography of area TEO in the macaque. *J Comp Neurol* 306:554–575.
- Bremmer F, Schlack A, Shah NJ, Zafiris O, Kubischik M, Hoffmann K, Zilles K, Fink GR (2001): Polymodal motion processing in posterior parietal and premotor cortex: A human fMRI study strongly implies equivalencies between humans and monkeys. *Neuron* 29:287–296.
- Brodmann K (1909): *Vergleichende Lokalisationslehre der Großhirnrinde*. Leipzig: Barth.
- Burkhalter A, Felleman DJ, Newsome WT, Van Essen DC (1986): Anatomical and physiological asymmetries related to visual areas V3 and VP in macaque extrastriate cortex. *Vision Res* 26: 63–80.
- Cavada C, Goldman-Rakic PS (1993): Multiple visual areas in the posterior parietal cortex of primates. *Prog Brain Res* 95: 123–137.
- Clarke S, Miklossy J (1990): Occipital cortex in man: Organization of callosal connections, related myelo- and cytoarchitecture, and putative boundaries of functional visual areas. *J Comp Neurol* 298:188–214.
- Clarke S, Maeder P, Meuli R, Staub F, Bellmann A, Regli L, de Tribolet N, Assal G (2000): Interhemispheric transfer of visual motion information after a posterior callosal lesion: A neuropsychological and fMRI study. *Exp Brain Res* 132:127–133.
- Conway BR, Tsao DY (2006): Color architecture in alert macaque cortex revealed by fMRI. *Cereb Cortex* 16:1604–1613.
- Desimone R, Schein SJ (1987): Visual properties of neurons in area V4 of the macaque: Sensitivity to stimulus form. *J Neurophysiol* 57:835–868.
- Desimone R, Ungerleider LG (1986): Multiple visual areas in the caudal superior temporal sulcus of the macaque. *J Comp Neurol* 248:164–189.
- DeYoe EA, Carman GJ, Bandettini P, Glickman S, Wieser J, Cox R, Miller D, Neitz J (1996): Mapping striate and extrastriate visual areas in human cerebral cortex. *Proc Natl Acad Sci USA* 93: 2382–2386.
- Dixon WJ, Brown MB, Engelman L, Hill MA, Jennrich RI (1988): *BMDP Statistical Software Manual*. Berkeley: University of California Press.
- Eickhoff S, Walters N, Schleicher A, Egan G, Watson J, Zilles K, Amunts K (2005b): High resolution MR imaging reveals microstructural features of the cerebral cortex. *Hum Brain Mapp* 24:206–215.
- Eickhoff SB, Stephan KE, Mohlberg H, Grefkes C, Fink GR, Amunts K, Zilles K (2005a): A new SPM toolbox for combining probabilistic cytoarchitectonic maps and functional imaging data. *Neuroimage* 25:1325–1335.
- Eickhoff SB, Amunts K, Mohlberg H, Zilles K (2006a): The human parietal operculum. II. Stereotaxic maps and correlation with functional imaging results. *Cereb Cortex* 16:268–279.
- Eickhoff SB, Heim S, Zilles K, Amunts K (2006b): Testing anatomically specified hypotheses in functional imaging using cytoarchitectonic maps. *Neuroimage* 32:570–582.
- Eickhoff SB, Schleicher A, Zilles K, Amunts K (2006c): The human parietal operculum. I. Cytoarchitectonic mapping of subdivisions. *Cereb Cortex* 16:254–267.
- Engel SA, Glover GH, Wandell BA (1997): Retinotopic organization in human visual cortex and the spatial precision of functional MRI. *Cereb Cortex* 7:181–192.
- Ettlinger G (1990): "Object vision" and "spatial vision": The neuropsychological evidence for the distinction. *Cortex* 26:319–341.
- Evans AC, Marrett S, Neelin P, Collins L, Worsley K, Dai W, Milot S, Meyer E, Bub D (1992): Anatomical mapping of functional activation in stereotaxic coordinate space. *Neuroimage* 1:43–53.
- Felleman DJ, Van Essen DC (1987): Receptive field properties of neurons in area V3 of macaque monkey extrastriate cortex. *J Neurophysiol* 57:889–920.
- Felleman DJ, Van Essen DC (1991): Distributed hierarchical processing in the primate cerebral cortex. *Cereb Cortex* 1: 1–47.

- Felleman DJ, Burkhalter A, Van Essen DC (1997): Cortical connections of areas V3 and VP of macaque monkey extrastriate visual cortex. *J Comp Neurol* 379:21–47.
- Fink GR, Marshall JC, Weiss PH, Stephan T, Grefkes C, Shah NJ, Zilles K, Dieterich M (2003): Performing allocentric visuospatial judgments with induced distortion of the egocentric reference frame: An fMRI study with clinical implications. *Neuroimage* 20:1505–1517.
- Fize D, Vanduffel W, Nelissen K, Denys K, Chef dC, Faugeras O, Orban GA (2003): The retinotopic organization of primate dorsal V4 and surrounding areas: A functional magnetic resonance imaging study in awake monkeys. *J Neurosci* 23:7395–7406.
- Foster KH, Gaska JP, Nagler M, Pollen DA (1985): Spatial and temporal frequency selectivity of neurones in visual cortical areas V1 and V2 of the macaque monkey. *J Physiol* 365:331–363.
- Gallant JL, Connor CE, Van Essen DC (1998): Neural activity in areas V1, V2 and V4 during free viewing of natural scenes compared to controlled viewing. *Neuroreport* 9:2153–2158.
- Gardner JL, Sun P, Waggoner RA, Ueno K, Tanaka K, Cheng K (2005): Contrast adaptation and representation in human early visual cortex. *Neuron* 47:607–620.
- Girard P, Lomber SG, Bullier J (2002): Shape discrimination deficits during reversible deactivation of area V4 in the macaque monkey. *Cereb Cortex* 12:1146–1156.
- Grefkes C, Geyer S, Schormann T, Roland P, Zilles K (2001): Human somatosensory area 2: Observer-independent cytoarchitectonic mapping, interindividual variability, and population map. *Neuroimage* 14:617–631.
- Grefkes C, Weiss PH, Zilles K, Fink GR (2002): Crossmodal processing of object features in human anterior intraparietal cortex: An fMRI study implies equivalencies between humans and monkeys. *Neuron* 35:173–184.
- Grill-Spector K, Kushnir T, Hendler T, Edelman S, Itzhak Y, Malach R (1998): A sequence of object-processing stages revealed by fMRI in the human occipital lobe. *Hum Brain Mapp* 6:316–328.
- Hadjikhani N, Liu AK, Dale AM, Cavanagh P, Tootell RB (1998): Retinotopy and color sensitivity in human visual cortical area V8. *Nat Neurosci* 1:235–241.
- Hasnain MK, Fox PT, Woldorff MG (1998): Intersubject variability of functional areas in the human visual cortex. *Hum Brain Mapp* 6:301–315.
- Haynes JD, Tregellas J, Rees G (2005): Attentional integration between anatomically distinct stimulus representations in early visual cortex. *Proc Natl Acad Sci USA* 102:14925–14930.
- Henn S, Schormann T, Engler K, Zilles K, Witsch K (1997): Elastische Anpassung in der digitalen Bildverarbeitung auf mehreren Auflösungsstufen mit Hilfe von Mehrgitterverfahren. In: Paulus E, Wahl FM, editors. *Mustererkennung 1997*. Wien: Springer. pp 392–399.
- Heim S, Alter K, Ischebeck AK, Amunts K, Eickhoff SB, Mohlberg H, Zilles K, von Cramon DY, Friederici AD (2005): The role of the left Brodmann's areas 44 and 45 in reading words and pseudowords. *Cogn Brain Res* 25:982–93.
- Hömke L (2006): A multigrid method for anisotropic PDE's in elastic image registration. *Numer Lin Algebra Appl* 13:215–229.
- Huk AC, Dougherty RF, Heeger DJ (2002): Retinotopy and functional subdivision of human areas MT and MST. *J Neurosci* 22:7195–7205.
- Hurlemann R, Matusch A, Eickhoff SB, Palomero-Gallagher N, Meyer P, Boy C, Maier W, Zilles K, Amunts K, Bauer A (2005): Analysis of neuroreceptor PET data based on cytoarchitectonic maximum probability maps—A feasibility study. *Anat Embryol* 210:447–453.
- Jones SE, Buchbinder BR, Aharon I (2000): Three-dimensional mapping of cortical thickness using Laplace's equation. *Hum Brain Mapp* 11:12–32.
- Kanwisher N, McDermott J, Chun MM (1997): The fusiform face area: A module in human extrastriate cortex specialized for face perception. *J Neurosci* 17:4302–4311.
- Kastner S, De Weerd P, Ungerleider LG (2000): Texture segregation in the human visual cortex: A functional MRI study. *J Neurophysiol* 83:2453–2457.
- Larsson J, Amunts K, Gulyas B, Malikovic A, Zilles K, Roland PE (2002): Perceptual segregation of overlapping shapes activates posterior extrastriate visual cortex in man. *Exp Brain Res* 143:1–10.
- Larsson J, Landy MS, Heeger DJ (2006): Orientation-selective adaptation to first- and second-order patterns in human visual cortex. *J Neurophysiol* 95:862–881.
- Li W, Piech V, Gilbert CD (2004): Perceptual learning and top-down influences in primary visual cortex. *Nat Neurosci* 7: 651–657.
- Lund JS (1988): Anatomical organization of macaque monkey striate visual cortex. *Annu Rev Neurosci* 11:253–288.
- Mahalanobis PC, Majumda DN, Rao DC (1949): Anthropometric survey of the united provinces. A statistical study. *Sankhya* 9:89–324.
- Malach R, Reppas JB, Benson RR, Kwong KK, Jiang H, Kennedy WA, Ledden PJ, Brady TJ, Rosen BR, Tootell RB (1995): Object-related activity revealed by functional magnetic resonance imaging in human occipital cortex. *Proc Natl Acad Sci USA* 92:8135–8139.
- Malach R, Levy I, Hasson U (2002): The topography of high-order human object areas. *Trends Cogn Sci* 6:176–184.
- Malikovic A, Amunts K, Schleicher A, Mohlberg H, Eickhoff SB, Wilms M, Palomero-Gallagher N, Armstrong E, Zilles K: Cytoarchitectonic analysis of the human extrastriate cortex in the region of V5/MT+: A probabilistic, stereotaxic map of area hOc5. *Cereb Cortex* (in press).
- McKeefry DJ, Zeki S (1997): The position and topography of the human colour centre as revealed by functional magnetic resonance imaging. *Brain* 120 (Part 12):2229–2242.
- Merigan WH (2000): Cortical area V4 is critical for certain texture discriminations, but this effect is not dependent on attention. *Vis Neurosci* 17:949–958.
- Merker B (1983): Silver staining of cell bodies by means of physical development. *J Neurosci Methods* 9:235–241.
- Merriam EP, Colby CL (2005): Active vision in parietal and extrastriate cortex. *Neuroscientist* 11:484–493.
- Mishkin M, Ungerleider LG (1982): Contribution of striate inputs to the visuospatial functions of parieto-preoccipital cortex in monkeys. *Behav Brain Res* 6:57–77.
- Mohlberg H, Lerch J, Amunts K, Evans AC, Zilles K (2003): Probabilistic cytoarchitectonic maps transformed into MNI space. Presented at the ninth international conference on functional mapping of the human brain, New York, June 18–22, 2003 (Poster No. 905).
- Moran J, Desimone R (1985): Selective attention gates visual processing in the extrastriate cortex. *Science* 229:782–784.
- Morosan P, Rademacher J, Schleicher A, Amunts K, Schormann T, Zilles K (2001): Human primary auditory cortex: Cytoarchitec-

- tonic subdivisions and mapping into a spatial reference system. *Neuroimage* 13:684–701.
- Naito E, Roland PE, Grefkes C, Choi HJ, Eickhoff S, Geyer S, Ehrsson HH (2005): Dominance of the right hemisphere and role of area 2 in human kinaesthesia. *J Neurophysiol* 93:1020–1034.
- Orban GA, Van Essen D, Vanduffel W (2004): Comparative mapping of higher visual areas in monkeys and humans. *Trends Cogn Sci* 8:315–324.
- Passingham RE, Stephan KE, Kotter R (2002): The anatomical basis of functional localization in the cortex. *Nat Rev Neurosci* 3:606–616.
- Roland PE, O'Sullivan B, Kawashima R (1998): Shape and roughness activate different somatosensory areas in the human brain. *Proc Natl Acad Sci USA* 95:3295–3300.
- Rosa MG, Manger PR (2005): Clarifying homologies in the mammalian cerebral cortex: The case of the third visual area (V3). *Clin Exp Pharmacol Physiol* 32:327–339.
- Sarkisov SA, Filimonoff IN, Preobrashenskaya NS (1949): [Cytoarchitecture of the human cortex cerebri]. Moscow: Medgiz (in Russian).
- Schira MM, Fahle M, Donner TH, Kraft A, Brandt SA (2004): Differential contribution of early visual areas to the perceptual process of contour processing. *J Neurophysiol* 91:1716–1721.
- Schleicher A, Amunts K, Geyer S, Kowalski T, Zilles K (1998): An observer-independent cytoarchitectonic mapping of the human cortex using a stereological approach. *Acta Stereologica* 17:75–82.
- Schleicher A, Amunts K, Geyer S, Morosan P, Zilles K (1999): Observer-independent method for microstructural parcellation of cerebral cortex: A quantitative approach to cytoarchitectonics. *Neuroimage* 9:165–177.
- Schleicher A, Amunts K, Geyer S, Kowalski T, Schormann T, Palomero-Gallagher N, Zilles K (2000): A stereological approach to human cortical architecture: Identification and delineation of cortical areas. *J Chem Neuroanat* 20:31–47.
- Schleicher A, Palomero-Gallagher N, Morosan P, Eickhoff SB, Kowalski T, de Vos K, Amunts K, Zilles K (2005): Quantitative architectural analysis: A new approach to cortical mapping. *Anat Embryol* 210:373–386.
- Schmitt O, Bohme M (2002): A robust transcortical profile scanner for generating 2-d traverses in histological sections of richly curved cortical courses. *Neuroimage* 16:1103–1119.
- Sereno MI, Dale AM, Reppas JB, Kwong KK, Belliveau JW, Brady TJ, Rosen BR, Tootell RB (1995): Borders of multiple visual areas in humans revealed by functional magnetic resonance imaging. *Science* 268:889–893.
- Sherman SM (2001): Thalamic relay functions. *Prog Brain Res* 134: 51–69.
- Smith AT, Cotillon-Williams NM, Williams AL (2006): Attentional modulation in the human visual cortex: the time-course of the BOLD response and its implications. *Neuroimage* 29:328–334.
- Tootell RB, Hadjikhani N (2001): Where is 'dorsal V4' in human visual cortex? Retinotopic, topographic and functional evidence. *Cereb Cortex* 11:298–311.
- Tootell RB, Mendola JD, Hadjikhani NK, Ledden PJ, Liu AK, Reppas JB, Sereno MI, Dale AM (1997): Functional analysis of V3A and related areas in human visual cortex. *J Neurosci* 17:7060–7078.
- Tsao DY, Vanduffel W, Sasaki Y, Fize D, Knutsen TA, Mandeville JB, Wald LL, Dale AM, Rosen BR, Van Essen DC, Livingstone MS, Orban GA, Tootell RB (2003): Stereopsis activates V3A and caudal intraparietal areas in macaques and humans. *Neuron* 39:555–568.
- Vanduffel W, Fize D, Mandeville JB, Nelissen K, Van HP, Rosen BR, Tootell RB, Orban GA (2001): Visual motion processing investigated using contrast agent-enhanced fMRI in awake behaving monkeys. *Neuron* 32:565–577.
- Van Essen DC, Zeki SM (1978): The topographic organization of rhesus monkey prestriate cortex. *J Physiol* 277: 193–226.
- Van Essen DC, Drury HA, Joshi S, Miller MI (2000): Functional and structural mapping of human cerebral cortex: Solutions are in the surfaces. *Adv Neurol* 84:23–34.
- Van Essen DC, Lewis JW, Drury HA, Hadjikhani N, Tootell RB, Bakircioglu M, Miller MI (2001): Mapping visual cortex in monkeys and humans using surface-based atlases. *Vision Res* 41:1359–1378.
- Victor JD, Purpura K, Katz E, Mao B (1994): Population encoding of spatial frequency, orientation, and color in macaque V1. *J Neurophysiol* 72:2151–2166.
- von Economo K, Koskinas G (1925): Die Cytoarchitektonik der Hirnrinde des erwachsenen Menschen. Wien: Springer.
- Wade AR, Brewer AA, Rieger JW, Wandell BA (2004): Functional measurements of human ventral occipital cortex: Retinotopy and colour. *Philos Trans R Soc Lond B Biol Sci* 357:963–973.
- Walters NB, Eickhoff S, Schleicher A, Zilles K, Amunts K, Egan GF, Watson JDG: Observer independent analysis of high-resolution MR images of the human cerebral cortex: In vivo delineation of cortical areas. *Hum Brain Mapp* (in press).
- Warnking J, Dojat M, Guerin-Dugue A, Delon-Martin C, Olympieff S, Richard N, Chehikian A, Segebarth C (2002): fMRI retinotopic mapping—step by step. *Neuroimage* 17:1665–1683.
- Weiss PH, Marshall JC, Wunderlich G, Tellmann L, Halligan PW, Freund HJ, Zilles K, Fink GR (2000): Neural consequences of acting in near versus far space: A physiological basis for clinical dissociations. *Brain* 123 (Part 12):2531–2541.
- Wilms M, Eickhoff SB, Specht K, Amunts K, Shah NJ, Malikovic A, Fink GR (2005): Human V5/MT+: Comparison of functional and cytoarchitectonic data. *Anat Embryol* 210: 485–95.
- Worgotter F, Eysel UT (2000): Context, state and the receptive fields of striatal cortex cells. *Trends Neurosci* 23:497–503.
- Wree A, Schleicher A, Zilles K (1982): Estimation of volume fractions in nervous tissue with an image analyzer. *J Neurosci Methods* 6:29–43.
- Young JP, Herath P, Eickhoff S, Choi J, Grefkes C, Zilles K, Roland PE (2004): Somatotopy and attentional modulation of the human parietal and opercular regions. *J Neurosci* 24:5391–5399.
- Zeki S, Watson JD, Lueck CJ, Friston KJ, Kennard C, Frackowiak RS (1991): A direct demonstration of functional specialization in human visual cortex. *J Neurosci* 11:641–649.
- Zeki S, McKeefry DJ, Bartels A, Frackowiak RS (1998): Has a new color area been discovered? *Nat Neurosci* 1:335–336.
- Zeki SM (1969a): Representation of central visual fields in prestriate cortex of monkey. *Brain Res* 14:271–291.
- Zeki SM (1969b): The secondary visual areas of the monkey. *Brain Res* 13:197–226.
- Zeki SM (1978a): Functional specialisation in the visual cortex of the rhesus monkey. *Nature* 274:423–428.

- Zeki SM (1978b): The third visual complex of rhesus monkey prestriate cortex. *J Physiol* 277:245–272.
- Zilles K, Clarke S (1997): Architecture, connectivity, and transmitter receptors of human extrastriate visual cortex. Comparison with nonhuman primates. In: Rockland KS, Kaas JH, Peters A, editors. *Cerebral Cortex*, Vol. 12. New York: Plenum Press. pp 673–742.
- Zilles K, Armstrong E, Schleicher A, Kretschmann HJ (1988): The human pattern of gyrification in the cerebral cortex. *Anat Embryol (Berl)* 179:173–179.
- Zilles K, Schleicher A, Palomero-Gallagher N, Amunts K (2002): Quantitative analysis of cyto- and receptor architecture of the human brain. In: Mazziotta J, Toga A, editors. *Brain Mapping: The Methods*. San Diego: Elsevier. pp 573–602.
- Zilles K, Eickhoff S, Palomero-Gallagher N (2003): The human parietal cortex: A novel approach to its architectonic mapping. *Adv Neurol* 93:1–21.
- Zilles K, Palomero-Gallagher N, Schleicher A (2004): Transmitter receptors and functional anatomy of the cerebral cortex. *J Anat* 205:417–432.